Few-Cycle THz Emission from Cold Plasma Oscillations

R. Kersting,[1] K. Unterrainer,[1] G. Strasser,[1] H. F. Kauffmann,[2] and E. Gornik[1]
[1]*Institut für Festkörperelektronik und Mikrostrukturzentrum der TU-Wien, Floragasse 7, A-1040 Wien, Austria*
[2]*Institut für Physikalische Chemie, Universität Wien, Währingerstrasse 42, A-1090 Wien, Austria*
(Received 12 April 1996)

We report on THz emission from plasma oscillations in semiconductors excited by femtosecond optical pulses. Time-resolved correlation measurements are performed on p-i-n and n-doped GaAs structures. In p-i-n structures coherent oscillations of the hot photogenerated carrier plasma emit THz radiation. A fundamentally new emission process is proposed in n-doped GaAs structures. Here, the screening of the surface field starts plasma oscillations of the cold electrons in the GaAs bulk leading to an efficient emission of few-cycle THz radiation. [S0031-9007(97)04294-4]

PACS numbers: 72.30.+q, 73.20.Mf, 78.47.+p

Since the first observation of THz emission from semiconductor surfaces excited by ultrafast laser pulses [1], considerable effort has been made both in understanding the mechanisms responsible for the THz generation, and in applications of these few-cycle THz pulses [2]. Subpicosecond and high intensity THz pulses have already been generated successfully [3,4] and applications range from measurement techniques in spectroscopy to high-resolution imaging [5].

Besides optical rectification of ultrafast laser pulses [1], two processes are known to contribute to the emission of THz radiation in bulk semiconductors. One source is the instantaneous polarization that arises during optical excitation when electron-hole pairs are generated in the electric field region of a semiconductor as, for example, in the depletion or surface field. A second emission process results from the transport of photoexcited carriers in the field region. The first process is attributed to coherent effects during optical excitation [6–8] and the latter to the motion of carriers, which includes ballistic transport and carrier drift [9]. In a recent work, Hu *et al.* investigated the THz emission processes with a high temporal resolution of 10 fs and have been able to separate clearly different steps like instantaneous polarization, ballistic transport, carrier drift, and the onset of intervalley transfer [10].

THz generation by ultrafast dynamic field screening has been the subject of a multitude of studies [2]. Recently, Sha *et al.* observed in optical pump and probe experiments on p-i-n structures oscillations of the built-in field which indicate coherent plasma oscillations of the photogenerated carriers [11]. Similar results were reported by Fischler *et al.* [12] and Cho *et al.* [13]. Such plasma oscillations should emit radiation in the THz regime. Thus, time-resolved measurements of this radiation are a direct probe of the underlying coherent carrier dynamics. Recently, Voßebürger *et al.* observed THz emission from a two-dimensional electron gas which was attributed to lateral plasma oscillations started by inverse Landau damping [14].

In this Letter we report on THz emission from coherent plasma oscillations vertical to the surface of bulk doped semiconductors. The THz emission results from the response of carriers to the field screening induced by the ultrafast photoexcitation. Our time-resolved measurements of the THz emission give insight into the dynamics of these plasma oscillations and their generation processes.

Our experiments are performed using a mode-locked Ti:Sapphire laser emitting 100 fs pulses at 800 nm (1.55 eV) with a pulse energy of 13 nJ. The pulses are transmitted through a Michelson interferometer and focused onto the sample to spot sizes between 100 and 500 μm at a polar angle of 45°. In the reflection geometry, the generated THz emission is collected by off-axis parabolic mirrors and focused onto a 4.2 K bolometer. The experimental setup is purged with nitrogen to prevent absorption by atmospheric moisture. All experiments are performed at 300 K.

Time resolution is achieved in our experiment by focusing two delayed laser pulses generated by the Michelson interferometer on the sample. In this correlation technique the time integrated THz signal emitted from the sample is detected with a bolometer as a function of the delay time between the two exciting pulses. The second pulse generates also an oscillating polarization if only partial field screening of the first exciting pulse is assumed. Since these polarizations are superimposed at the bolometer, the detected cw signal depends on the phase difference between the oscillations which is given by the time delay between the two laser pulses.

Two sets of GaAs structures were fabricated for our experiment: p-i-n structures and n-doped epilayers, both grown by molecular beam epitaxy. The p-i-n structure was grown on a p^+-doped substrate followed by a 1.4 μm layer intrinsic GaAs, 35 nm of 1.5×10^{18} cm^{-3} n-doped GaAs, and a cap layer of 5 nm undoped GaAs. In the intrinsic region the built-in field is estimated to be 10 kV/cm. The n-doped samples were grown on semi-insulating substrates with corresponding epilayer thicknesses of 3.7, 2.0, and 1.8 μm. The doping densities

 0031-9007/97/79(16)/3038(4)$10.00

are determined by standard Hall measurements and are corrected for the depletion layer thickness yielding concentrations of 1.9×10^{15} cm^{-3}, 1.7×10^{16} cm^{-3}, and 1.1×10^{17} cm^{-3}, respectively.

Correlation data recorded on the *p-i-n* structure after femtosecond excitation are shown in Fig. 1. The inset shows the corresponding amplitude spectrum deduced by Fourier transformation. The correlation data display a strongly damped oscillation. For all excitation densities investigated the widths of the correlation functions are broader than the pulse duration of the exciting laser. Thus, we can exclude contributions from optical rectification by nonlinear optical χ^2 processes. This finding is supported by the absence of any crystallographic dependence of the signal intensities on the azimuth angle of the laser pulses [15,16]. However, the THz radiation possesses a small beam divergence of about 4° FWHM indicating the spatial coherence of the radiation.

In accordance with literature (see, e.g., [2,10,17]) we explain the experimental data by the screening of the built-in field by photogenerated carriers. The photocarriers are generated within the field region between the *n*-doped and *p*-doped layers. The initial acceleration of the photogenerated electrons and holes in the built-in field induces a polarization. This acts as the restoring force of the carrier motion. As a consequence, the photo carriers undergo subsequent plasma oscillations with the frequency $\omega = \sqrt{\omega_p^2 - \gamma^2/4}$ which is determined by the damping rate γ and the plasma frequency

$$\omega_p = \sqrt{\frac{ne^2}{\epsilon\epsilon_0 m^*}}. \qquad (1)$$

Here, n is the density of coherently oscillating carriers and m^* is the reduced effective mass. In a previous paper, Sha *et al.* [11] showed that the internal field of such a *p-i-n* diode indeed oscillates at the plasma frequency. Thus, we attribute the observed THz emission from our *p-i-n* sample to the coherent oscillation of photogenerated carriers. This proposal is supported by the dependence of the peak emission frequencies on excitation density shown in Fig. 2. The frequencies were estimated by Fourier transformation of the correlation data and by fitting the spectra to a Lorentzian profile (the error bars depict the error in the peak frequency, rather than the width of the Fourier spectra). The emission frequencies show the expected square root dependence of the plasma frequency on the excitation density. This dependence is direct evidence that the photogenerated carriers perform plasma oscillations. However, the measured values are smaller than expected from Eq. (1). In part, this may be caused by the experimental uncertainty in the absolute values of the excitation density and by local field screening by accumulation of photogenerated carriers.

We observed a different emission process in *n*-doped structures. Time-resolved data from these samples are shown in Fig. 3. In contrast to the data recorded on the *p-i-n* structure, multiple oscillations are clearly visible at higher doping concentrations. These data show features that are incompatible with the picture of emission from hot plasma oscillations of photogenerated carriers: The oscillation period depends on the doping concentration and does not show any dependence on the density of photogenerated carriers (see Fig. 2). In addition, the emission of optical phonons should cause a faster damping of the oscillations when the excess energy of the photogenerated carriers is increased. However, this is not observed in our experiment performed with different excitation wavelengths. These results indicate that a new mechanism is required for the observed emission process.

We explain the experimental results in the following framework. In *n*-doped structures cold electrons are confined by the surface depletion layer on one side and by the electric field at the interface between the epilayer and the substrate on the other side. After excitation the photogenerated carriers screen the surface field. Since the cold electron plasma responds to the field change

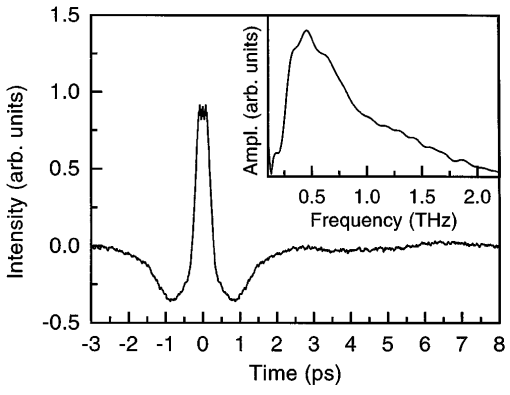

FIG. 1. Correlation data recorded on the *p-i-n* structure at room temperature. The excitation density is $n_{exc} = 1.1 \times 10^{16}$ cm^{-3}. The inset shows the corresponding Fourier spectrum.

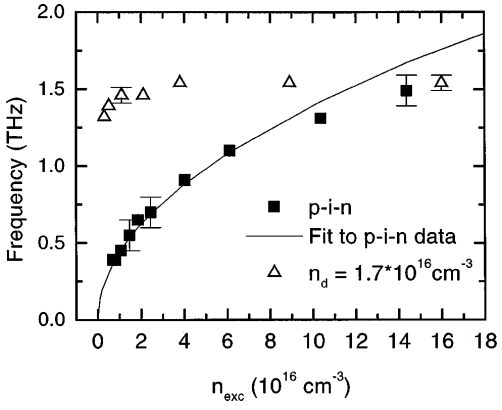

FIG. 2. Oscillation frequencies of the *p-i-n* structure (squares) and of the sample with a doping of 1.7×10^{16} cm^{-3} (triangles) in dependence on the excitation density. The solid line shows a square root fit to the data of the *p-i-n* structure.

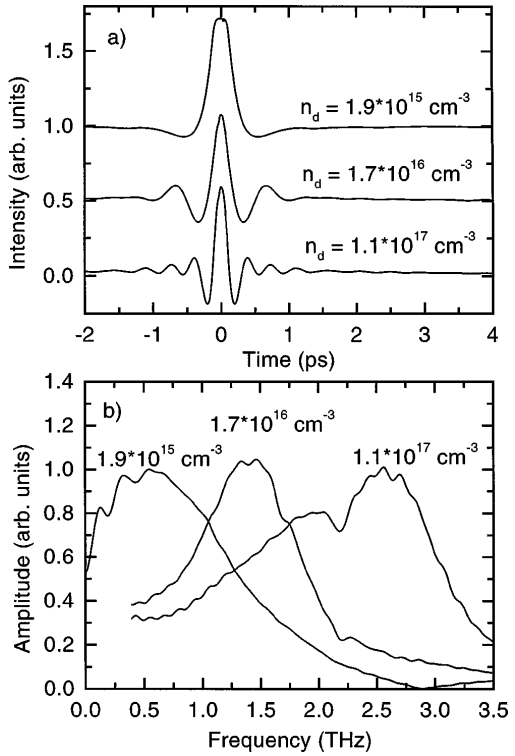

FIG. 3. (a) Correlation data recorded on n-doped GaAs structures. The excitation density is always smaller than the doping concentration. (b) Corresponding Fourier spectra. The broad absorption line at 2.25 THz results from the polyethylene window of the bolometer.

at the edge of the depletion zone the single-sided surface screening is the starting mechanism of the cold plasma oscillations. This interpretation is supported by the experimental findings that (i) the observed frequencies depend on the doping density of the n-doped layer, (ii) the observed frequencies are independent on the excitation density, and (iii) oscillation frequencies and damping times are independent on the excitation wavelength.

The interpretation in terms of the single-sided field screening is confirmed by measurements of the intensities of the generated THz pulses. In these experiments the delay between the exciting laser pulses was set to 5 ps. At this time delay, the interference of the two THz pulses is negligible. The power of the THz radiation generated by the second laser pulse was compared with the power produced by the first pulse. While at low excitation densities the second pulse produces nearly the same power as the first one, the ratio decreases at excitation densities close to the doping concentration. The reason is because at high densities, the depletion field is completely screened by carriers excited by the first laser pulse. Thus, the second laser pulse cannot generate a plasma oscillation of similar amplitude and the emission is reduced. This result shows that field screening is the starting mechanism of the cold plasma oscillations. An alternative interpretation of the starting mechanism in terms of a momentum transfer from photogenerated carriers to the cold carrier plasma can be ruled out. Such a transfer would generate plasma oscillations with large wave vector which cannot radiate and are therefore not observable in our experiments.

For a more quantitative analysis we compared our measured data to model calculations. These simulations consist of the calculation of the field screening by the photogenerated carriers and of initiated response of the cold electron plasma. To calculate the field screening we adopt a drift-diffusion model developed by Dekorsy [18]. In this model, the spatial distributions of the carrier densities are calculated by

$$\frac{N_i(z,t)}{\partial t} = G(z,t) + \frac{\partial}{\partial z}\left\{D_i(z,t)\,\frac{\partial N_i(z,t)}{\partial z}\right\} \pm \frac{\partial}{\partial z}\left\{\mu_i(z,t)E(z,t)N_i(z,t)\right\}, \quad (2)$$

where $N_i(z,t)$, μ_i, and D_i are, respectively, the carrier concentration, mobility, and diffusion constant for either electrons or holes. $G(z,t)$ is the carrier generation by the laser pulse. The electric field $E(z,t)$ is calculated self-consistently from the carrier densities of photogenerated electrons N_e, holes N_h, and the doping concentration N_d:

$$\frac{\partial E(z,t)}{\partial z} = \frac{q}{\epsilon\epsilon_0}\left[N_h(z,t) - N_e(z,t) \pm N_d(z,t)\right]. \quad (3)$$

A more detailed description of the model will be found in [18,19].

Since the drift-diffusion model yields the transient of the electric field $E(z,t)$, the response of the cold plasma can be calculated by the simulation of a driven oscillator. Figure 4(a) shows the transient of the surface field at the edge of the depletion zone and the response of the cold electron plasma. The far field emitted by the cold plasma oscillation can be deduced from $E_{\mathrm{rad}} \sim \frac{\partial^2}{\partial t^2} z$. Autocorrelations of the THz radiation emitted by the oscillation of the cold plasma are shown in Fig. 4(b) together with the experimental data recorded on the sample with a carrier concentration of $n_d = 1.7 \times 10^{16}$ cm^{-3}. We found a good agreement between experiment and simulation if we assume a plasma frequency of 1.5 THz and a damping rate $\gamma = 5$ ps^{-1}. For the sample with $n_d = 1.1 \times 10^{17}$ cm^{-3} we found a plasma frequency of 2.8 THz and a damping rate of 6.5 ps^{-1}.

The measured damping rates γ merit further discussion. In n-doped structures the damping of plasma oscillations is given by: (i) optical phonon scattering and (ii) first-order single particle interactions, i.e., Landau damping [20]. Carrier-carrier-scattering between hot and cold carriers conserves the momentum of the plasmon and can be ruled out. Landau damping includes both elastic and inelastic electron-electron scattering. However, Landau damping is suppressed if the excited plasmon wave vector lies outside of the single particle excitation continuum [20]. This is the case in our experiments since the

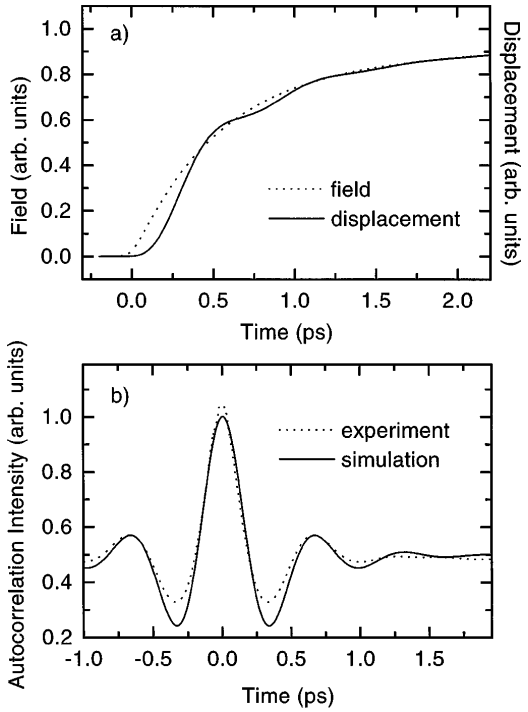

FIG. 4. (a) Calculated field change at the end of the depletion zone and response of the cold carrier plasma in a structure with a n-doping of 1.7×10^{16} cm^{-3}. (b) Comparison of simulated autocorrelation data and experimental data.

wave vector of the plasmon is nearly zero and orders of magnitude smaller than the "onset" wave vector for Landau damping [21]. This inhibits both the decay of the excited cold plasmon into single particle excitations and its interaction with the hot photogenerated carriers. Thus, we expect that LO phonon scattering of the electrons is the dominant plasma damping mechanism. We compare our measured damping times to the scattering rates estimated from the dc mobilities which are phonon limited at room temperature. The corresponding scattering rates are $\gamma_{\mathrm{dc}} = 3.75$ ps^{-1} and 6.7 ps^{-1} for the doping concentrations of 1.7×10^{16} cm^{-3} and 1.1×10^{17} cm^{-3}, respectively. The observed plasmon damping times agree quite well with the dc scattering rates which strongly suggests that phonon scattering is the dominant damping mechanism of the cold plasma oscillations.

In conclusion, we have investigated the generation process of few-cycle THz radiation in GaAs structures. The emission frequencies of p-i-n structures are found to depend on the excitation density, indicating that the observed THz signal results from the oscillation of hot photogenerated carriers in the intrinsic region. A new coherent emission process is found in n-doped samples. Here, the THz emission results from the oscillations of cold electrons in the bulk of the doped sample induced by the dynamic screening of the surface field. The generated frequencies of the THz radiation depend only on the doping concentration and range from 0.5 to 3 THz. The damping mechanism of the cold plasma oscillations is identified as being due to phonon scattering.

We thank G. C. Cho and J. N. Heyman for many fruitful discussions. We would like to acknowledge financial support by the Austrian Science Foundation, Vienna (START Y47-PHY and P9799–PHY) and the Gesellschaft für Mikroelektronik (GMe).

[1] X.-C. Zhang, B. Hu, J. Darrow, and D. Auston, Appl. Phys. Lett. **56**, 1011 (1990).
[2] In Special Issue on Terahertz Electromagnegtic Pulse Generation, Physics, and Applications, edited by D. Dykaar and S. Chuang [Optics Letters, **11**, 2457–2585 (1994)], and references therein.
[3] B. Greene *et al.*, Appl. Phys. Lett. **59**, 893 (1991).
[4] B. Hu *et al.*, Appl. Phys. Lett. **56**, 886 (1990).
[5] B. Hu and M. Nuss, in *Proceedings of the 15th Conference on Lasers and Electrooptics, Baltimore, 1995* (Optical Society of America, Washington, 1995) (postdeadline Report No. CPD44-1, 1995).
[6] E. Yablonovitch, J. Heritage, D. Aspnes, and Y. Yafet, Phys. Rev. Lett. **63**, 976 (1989).
[7] B. Hu, X.-C. Zhang, and D. Auston, Phys. Rev. Lett. **67**, 2709 (1991).
[8] A. Kuznetsov and C. Stanton, Phys. Rev. B **48**, 10 828 (1993).
[9] B. Hu *et al.*, Phys. Rev. B **49**, 2234 (1994).
[10] B. Hu *et al.*, Phys. Rev. Lett. **74**, 1689 (1995).
[11] W. Sha, A. Smirl, and W. Tseng, Phys. Rev. Lett. **74**, 4273 (1995).
[12] W. Fischler, P. Buchberger, R. A. Höpfel, and G. Zandler, Appl. Phys. Lett. **68**, 2778 (1996).
[13] G. C. Cho *et al.*, Phys. Rev. Lett. **77**, 4062 (1996).
[14] M. Voßebürger *et al.*, J. Opt. Soc. Am. B **13**, 1045 (1996).
[15] A. Rice *et al.*, Appl. Phys. Lett. **64**, 1324 (1994).
[16] A. Bonvalet, M. Joffre, J. Martin, and A. Mingus, Appl. Phys. Lett. **67**, 2907 (1995).
[17] A. Weling, B. Hu, N. Froberg, and D. Auston, Appl. Phys. Lett. **64**, 137 (1994).
[18] T. Dekorsy, T. Pfeifer, W. Kütt, and H. Kurz, Phys. Rev. B **47**, 3842 (1993).
[19] Details of the calculations and details of minor modifications for our purpose will be published in a forthcoming work.
[20] See, e.g., B. K. Ridley, *Quantum Processes in Semiconductors* (Oxford Science Publications, Clarendon Press, Oxford, 1993).
[21] H. Sato and Y. Hori, Phys. Rev. B **36**, 6033 (1987).